

Green Chemistry for Biomimetic Materials: Synthesis and Electrospinning of High-Molecular-Weight Polycarbonate-Based Nonisocyanate Polyurethanes

Dmitri Visser,* Hadi Bakhshi,* Katharina Rogg, Ellena Fuhrmann, Franziska Wieland, Katja Schenke-Layland, Wolfdietrich Meyer, and Hanna Hartmann



Cite This: *ACS Omega* 2022, 7, 39772–39781



Read Online

ACCESS |



Metrics & More

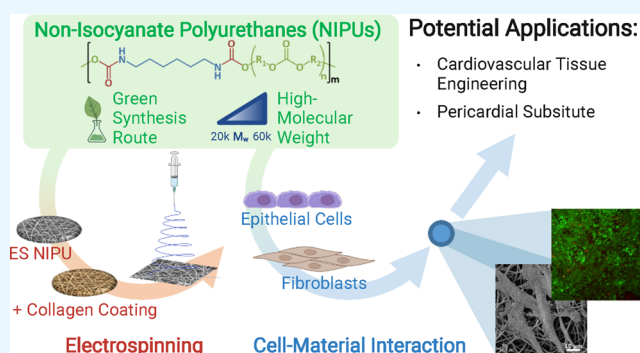


Article Recommendations



Supporting Information

ABSTRACT: Conventional synthesis routes for thermoplastic polyurethanes (TPUs) still require the use of isocyanates and tin-based catalysts, which pose considerable safety and environmental hazards. To reduce both the ecological footprint and human health dangers for nonwoven TPU scaffolds, it is key to establish a green synthesis route, which eliminates the use of these toxic compounds and results in biocompatible TPUs with facile processability. In this study, we developed high-molecular-weight nonisocyanate polyurethanes (NIPUs) through transurethanization of 1,6-hexanedicarbamate with polycarbonate diols (PCDLs). Various molecular weights of PCDL were employed to maximize the molecular weight of NIPUs and consequently facilitate their electrospinnability. The synthesized NIPUs were characterized by nuclear magnetic resonance, Fourier-transform infrared spectroscopy, gel permeation chromatography, and differential scanning calorimetry. The highest achieved molecular weight (M_w) was 58,600 g/mol. The NIPUs were consecutively electrospun into fibrous scaffolds with fiber diameters in the submicron range, as shown by scanning electron microscopy (SEM). To assess the suitability of electrospun NIPU mats as a possible biomimetic load-bearing pericardial substitute in cardiac tissue engineering, their cytotoxicity was investigated in vitro using primary human fibroblasts and a human epithelial cell line. The bare NIPU mats did not need further biofunctionalization to enhance cell adhesion, as it was not outperformed by collagen-functionalized NIPU mats and hence showed that the NIPU mats possess a great potential for use in biomimetic scaffolds.



1. INTRODUCTION

Thermoplastic polyurethanes (TPUs) are linear segmented polymers with a wide range of applications because of their superior mechanical properties and feasible processability. TPUs are generally synthesized through the reaction of isocyanates, polyols, and chain extenders, in the presence of tin-based catalysts. The principal limitation of this route is the high toxicity of isocyanate compounds causing irreversible environmental and human health damage.^{1–3} Isocyanates are not completely consumed during the polymerization process, and traces of isocyanate residues were detected in the final polyurethanes.^{4,5} Tin-based catalysts, for example, dibutyl-tin-dilaurate (DBTDL), are not removed after the polymerization process and can result in toxicity.^{6,7} Therefore, synthesis routes for TPUs excluding isocyanates and tin-based catalysts have attracted great interest, especially for the fabrication of biomedical materials,^{8–10} food packaging,^{11,12} and children products.

One route for synthesizing nonisocyanate polyurethanes (NIPUs) is through the transurethanization reaction between bis-carbamates and polyols, leading to a structure and

characteristics similar to classic TPUs but through solvent-free and green chemistry.^{13–15} TPUs can be synthesized using polyether, polyester, or polycarbonate (PC) polyols. PC-based TPUs exhibit superior hydrolysis and oxidation resistance, biostability, and biocompatibility compared to the polyether- and polyester-based ones and consequently have greater potential for long-term biomedical applications.¹⁶

Electrospinning is a versatile technique to process a wide variety of polymers into fibrous mats.¹⁷ Typically, a charged jet of polymer melt or solution is induced by a strong electric field and driven in a spinning motion toward a metal collector, while the jet solidifies. Electrospinning allows for the fabrication of nonwoven fibrous materials with fiber diameters ranging from

Received: June 15, 2022

Accepted: October 14, 2022

Published: October 26, 2022



tens of nanometers to several microns. As such, this technique has found its way into many applications, especially the production of functional materials that require an extremely high surface-to-volume ratio, such as sensors^{18–20} and filtration membranes.^{21,22} In the last two decades, the interest in the electrospinning technique for biomedical applications surged because of the high resemblance of mechanical and structural properties of electrospun materials to those of native tissues.^{23–26}

The highly variable chemistry of TPUs allows for tailored physio-chemical and biodegradable properties.^{27,28} Especially for long-term implants, TPUs have a long-standing reputation as biomaterials with good biocompatibility, which do not elicit inflammatory reactions. Additionally, the anti-thrombogenic properties of TPUs make them excellent biomaterials that come into contact with blood.²⁸ This has led to the investigation of electrospun TPUs as tissue-engineered vascular grafts,^{29–33} heart valves,^{34–36} and cardiac patches.^{37–39} However, most studies have only considered the electrospinning of TPUs based on isocyanate synthesis. Although water-soluble polymers have successfully raised the bar in making electrospinning more environmentally friendly, green electrospinning of NIPUs is still uncharted territory. Aduba et al.⁸ recently reported the electrospinning of polyether-based NIPUs, which were synthesized from cyclic carbonate methyl esters, and their potential for biomedical applications. To our knowledge, the present study is the first to present the electrospinning of PC-based NIPUs, which more closely resemble the classical TPUs.

This work aimed to synthesize high-molecular-weight PC-based NIPUs using nontoxic chemicals and green procedures, which are suitable for the electrospinning process as well as to establish and optimize the electrospinning process to obtain bead-free fibers with potential for biomedical applications. The NIPUs were synthesized by employing 1,6-hexanedicarbamate (1,6-HDC) as a green substitute for diisocyanates. The synthesized NIPUs were fully characterized before electrospinning and after electrospinning in biological tests.

2. EXPERIMENTAL SECTION

2.1. Materials. 1,6-Hexanediamine (1,6-HDA, 99.5%), dimethyl carbonate (DMC, 99%), sodium acetate, absolute methanol, chloroform, tetra butyl titanate (TBT), *N,N*-dimethylformamide (DMF), and sodium carbonate were obtained from Sigma Aldrich. Tetrahydrofuran (THF, 99.9%) was obtained from Carl Roth. Eternacoll UH50 (PCDL500, OH#: 224, 500 g/mol), Eternacoll UH100 (PCDL1000, OH#: 110, 1000 g/mol), and Eternacoll UH200 (PCDL2000, OH#: 56, 2000 g/mol) as aliphatic polycarbonate diols (PCDLs) were kindly supplied from UBE Corporation Europe. 1,1,1,3,3,3-Hexafluoroisopropanol (HFIP) was obtained from Iris Biotech GmbH.

2.2. Synthesis of 1,6-HDC. 1,6-HDC was synthesized from DMC and 1,6-HDA according to a reported procedure⁴⁰ with some modifications. 1,6-HDA (23.24 g, 200 mmol), DMC (18.02 mL, 400 mmol), sodium acetate (4.00 g, 48.8 mmol), and absolute methanol (100 mL) were added in a 500 mL three-neck round-bottomed flask equipped with a condenser, a magnetic stirrer, and an Ar inlet. The temperature was raised to 75 °C and the reaction mixture was stirred overnight. Over time, white floccules disappeared and turned the clear reaction mixture into a white dispersion. After cooling to room temperature, the reaction mixture was diluted with an

excess amount of HCl solution (2 N, 400 mL) and extracted with chloroform twice. The chloroform phases were combined and washed with distilled water. Removal of chloroform on a vacuum rotary evaporator yielded a white solid, which was purified through the recrystallization from the methanol/water mixture (1/1, 100 mL) at 80 °C and vacuum-drying overnight (23.45 g, 50% yield).

2.3. Transurethanization Polymerization. NIPUs were synthesized through the transurethanization reaction of PCDLs and 1,6-HDC according to a reported procedure⁸ with some modifications. PCDLs (43.0 mmol), 1,6-HDC (43.0 mmol), and TBT (0.2–0.3 wt %) were added in a 100 mL three-neck round-bottomed flask equipped with a condenser, a mechanical stirrer, an N₂ inlet, and a vacuum outlet. The mixture was heated at 170 °C and stirred mechanically to form a homogeneous melt, first under an N₂ atmosphere and then under reduced pressure. Later, the reaction mixture was transferred to a vacuum oven and heated at 170 °C under a dynamic vacuum. The reaction parameters for selected samples are summarized in Table S1. The product was dissolved in DMF (80 mL) at 70 °C, precipitated in methanol (2 L), and dried in a vacuum oven at 40 °C overnight.

2.4. Electrospinning of NIPUs. NIPUs were dissolved in DMF, THF, or HFIP at various concentrations (20–50 wt %) and temperatures up to 50 °C under stirring. For selected experiments, the conductivity of solutions was adjusted to 10 μS/cm by the supplementation of sodium carbonate,⁴¹ as measured with a conductivity meter (GMH 3431-LTG, Greisinger). The electrospinning process was done using a climate-controlled EC-CLI electrospinning setup (IME Technologies) with a flat collector plate, which allows for temperature control between 20 and 45 °C. All experiments were conducted with a 21G cannula corresponding to an inner diameter of 0.5 mm. The temperature and the relative humidity of the electrospinning chamber were kept at 35 °C and 20%, respectively, for all experiments. The remaining electrospinning parameters (voltage, flow rate, and tip-to-collector distance) were varied until a stable, fiber-yielding process was established. After electrospinning, the fibrous mats were dried in a vacuum oven at <5 mbar overnight to remove all solvent residues.

2.5. Instruments. Fourier transform infrared (FTIR) spectroscopy was done using a Thermo Fisher Scientific instrument (Nicolet iS20) equipped with an attenuated total reflection (ATR) unit (PIKE Technologies, GladiATR).

An nuclear magnetic resonance (NMR) spectrometer (Varian, Unity Inova 500 NB) was employed for recording the ¹H- and ¹³C-NMR spectra at 25 °C using CDCl₃ and DMF-*d*₇ as solvents.

The molecular weight distributions of samples were determined by gel permeation chromatography (GPC) in DMF containing LiBr (0.1%) using PSS GRAM Guard (8 × 50 mm), PSS GRAM 1000 Å (300 × 7.5 mm), PSS GRAM 1000 Å (300 × 7.5 mm), and PSS GRAM 30 Å (300 × 7.5 mm) columns (PSS Polymer Standards Service) and an SEC-3010 reflect index detector (WGE Dr. Bures GmbH) with a flow rate of 1 mL/min at 50 °C. The data were evaluated by ParSEC CPC/SEC software (Brookhaven Instruments) using polystyrenes with molecular weights of 265–2,570,000 g/mol (PSS Polymer Standards Service) as the standards.

A differential scanning calorimetry (DSC) instrument (Netzsch, DSC 204 F1 Phoenix) operating in a range of –50 to 200 °C with a heating rate of 10 °C/min under a N₂

atmosphere was used to study the thermal transition of samples. The glass transition (T_g), crystallization (T_c), cold crystallization (T_{cc}), and melting (T_m) temperatures were extracted from the middle point of the baseline change and corresponding peak maximums, respectively, in the second heating cycle.

The morphology of the electrospun NIPU mats was studied on a scanning electron microscopy (SEM) instrument (Zeiss, Auriga 40) operating at an electron gun voltage of 3 kV using a secondary electron detector. The mats were coated with gold–palladium in a sputtering system (Balzers, SCD-040) for 20 s before microscopy. Cell-loaded mats were fixed in a three-step process; first with paraformaldehyde (PFA, 4%) in Dulbecco's phosphate-buffered saline (DPBS) for 30 min, thereafter in PFA (4%) and glutaraldehyde (2%) in DPBS for 1 h, and consequently dehydrated with isopropanol through critical point drying. Fiber diameters were assessed in MATLAB using an adapted version of the Simpoly algorithm from Murphy et al.⁴² The source code of the used algorithm is available online at github.com/dvtxc/fibresem.

The surface hydrophilicity of the electrospun NIPU mats was assessed by measuring the water contact angle with the DSA25 drop-shape analyzer (Krüss). A photograph was taken 20 s after applying 2 μ L of deionized water onto the mats.

2.6. Biofunctionalization. The biofunctionalization of the electrospun NIPU mats was performed with rat tail collagen, type I (rCol I). Collagen was extracted from rat tail tendons using acid-based isolation and lyophilized for long-term storage. The collagen integrity after extraction was confirmed with electrophoretic assays and circular dichroism. Before biofunctionalization, the collagen lyophilisate was solubilized in acetic acid (0.1 M) at a concentration of 0.1 mg/mL. The mats were incubated in the collagen solution at 37 °C for 2 h before aspirating the excess solution and left to dry at 4 °C overnight. The collagen functionalization was confirmed with contact angle measurements and immunohistochemical staining against collagen I.

2.7. Biocompatibility Assays. The MTT assay was done to study the cytotoxicity of NIPU granulates and electrospun NIPU mats according to ISO 10993-5 and ISO 10993-12 norms. NIPU granulates were tested as obtained after the polymerization. Mats were dried in a vacuum at 50 °C and <5 mbar to remove all HFIP residues. Additional mats were washed three times in phosphate-buffered saline (PBS) for 10 min. Samples were incubated in the supplemented media at an extraction ratio of 3 cm²/mL. The L929 cells were cultured in minimal essential media supplemented with fetal bovine serum (FBS, 10%, 10270-106, Gibco), L-glutamine (4 mM, 2051024, Gibco), and penicillin–streptomycin (1%, 15070-063, Gibco) at 37 °C in a 5% CO₂ atmosphere. The cell viability was assessed with 1 mg/mL 3-(4,5-dimethylthiazol-2-yl)-2,5-diphenyltetrazolium bromide (MTT, M2128, Sigma-Aldrich) by measuring the absorbance at 570 nm with respect to the absorbance of the blank samples. The samples were considered to be cytotoxic when the relative cell viability was less than 70%. The positive control was a polyurethane film containing 0.1% zinc diethyldithiocarbamate (ZDEC, Hatano Research Institute) and the negative control was a high-density polyethylene (HDPE) film (Hatano Research Institute). All samples were prepared in triplicates.

The live/dead staining was performed to investigate the direct impact of the electrospun NIPU mats on the cells. The mats were punched, UV-sterilized (150 s, GS Gene Linker,

Bio-rad), washed three times with PBS, clamped in 24 well cell crowns (Sigma), and placed in 24-well plates (Corning). Primary human dermal fibroblasts (hDF) were isolated from foreskin biopsies under the ethics approval no 495/2018BO2 and cultured in Dulbecco's modified Eagle's medium (DMEM) supplemented with FBS (10%), L-Glutamine (4 mM), sodium pyruvate (1 mM), and penicillin–streptomycin (1%, ThermoFisher). Human epithelial cells (MeT-5A, ATCC) from the pleural mesothelium were cultured in the DMEM/F12 medium (ThermoFisher) supplemented with FBS (10%) and penicillin–streptomycin (1%). Both cell types were cultured at 37 °C in a 5% CO₂ atmosphere. Cells were removed from cell culture flasks with trypsin/EDTA (0.25%) and their concentration was adjusted so 4 × 10⁴ hDFs or 6 × 10⁴ MeT-5A cells were seeded on each mat. The positive control (nonadherent) was Parafilm as a highly hydrophobic surface and the negative control was glass. After 24 h or 7 days, the live/dead staining was done with calcein (Invitrogen) and propidium iodide (PI, Sigma-Aldrich) serving as the live and dead markers, respectively. All samples were prepared in triplicates.

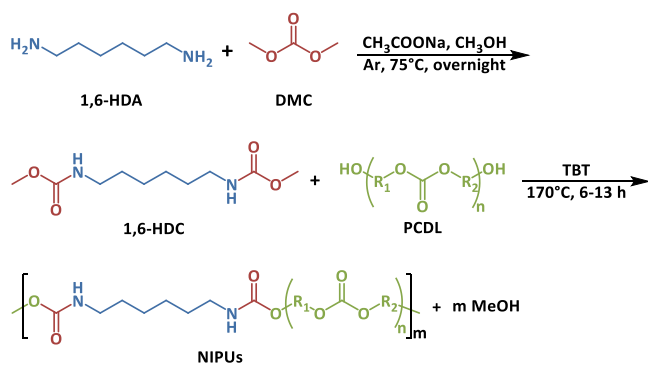
Immunohistochemical staining was done to assess the adhesion of collagen I on the biofunctionalized electrospun NIPU mats. Briefly, the biofunctionalized mats were blocked for 30 min with goat block, that is, goat serum (2%), Triton X-100 (0.1%), Tween 20 (0.05%), cold-water fish skin gelatine (0.1%), and bovine serum albumin (BSA, 1%) in DPBS, washed three times with Tween 20 in DPBS (0.05%), and incubated with a mouse anti-Col I primary antibody (1:500) at 4 °C overnight in DPBS buffer containing Triton X-100 (0.1%), Tween 20 (0.05%), cold-water fish skin gelatine (0.1%), and BSA (1%). Immunofluorescence labeling was performed with a goat anti-mouse IgG Alexa-Fluor 546 secondary antibody (1:250) for 30 min at room temperature in the same buffer as the primary antibody. Bare mats served as a control. To test for unspecific binding of the secondary antibody, a control without the primary collagen antibody was included as well. Samples were imaged through a 20× objective with a spinning disk laser microscope (Zeiss). Mean gray-value intensities (GVI) of three images per sample were extracted with ImageJ software.

3. RESULTS AND DISCUSSION

3.1. Polymerization of NIPUs. In general, two bis-carbamates are utilized for the transurethanization reaction; (1) bis-hydroxyalkylcarbamate formed by the reaction of ethylene carbonate with diamines¹⁴ and (2) bis-alkylcarbamate generated from the reaction of DMC with diamines.^{13,15} In this study, a bis-methylcarbamate, 1,6-HDC, was prepared from the reaction of DMC and 1,6-HDA (Scheme 1). 1,6-HDC was later reacted with PCDLs using TBT as a catalyst at 170 °C to prepare NIPUs through the transurethanization reaction.

To facilitate the electrospinning process, the resulting NIPU should also have a sufficiently high molecular weight. Therefore, several NIPUs were synthesized employing PCDLs with different molecular weights (500, 1000, and 2000 g/mol) at various stoichiometry ratios, TBT concentrations, temperatures, and vacuum pressures. Generally, PCDLs and 1,6-HDC were heated at 170 °C and stirred mechanically to form a homogeneous melt, first under an N₂ atmosphere and then under a vacuum. Later, the reaction mixture was transferred to a vacuum oven and heated at 170

Scheme 1. Synthesis Route for NIPUs



°C under a dynamic vacuum. The reaction parameters for selected samples are summarized in Table S1.

The molecular weights of NIPUs were evaluated via GPC (Table 1). The transurethanization reaction between PCDLs and 1,6-HDC generated methanol as a by-product, which should be eliminated from the reaction mixture to reach high-molecular-weight NIPUs. Initially, the reaction mixture was stirred mechanically under an atmospheric pressure for 3–4 h and then kept in a vacuum oven for 2–3 h, which led to a higher molecular weight for NIPU-A, based on PCDL500, compared to NIPU-B and NIPU-C, based on PCDL1000 and PCDL2000 (Table 1). The low viscosity of PCDL500 (100 cP at 75 °C) compared to PCDL1000 and PCDL2000 (410 and 2300 cP at 75 °C) resulted in a low viscous reaction mixture, which facilitated the removal of methanol and consequently the yield of the transurethanization reaction. To further improve the elimination of methanol and hence the molecular weight of NIPUs, the reaction mixtures were stirred under vacuum pressure (600 mbar) for another hour, which led to NIPU-D with almost double molecular weight compared to NIPU-A.

It is worth mentioning that employing stronger vacuums could vaporize the unreacted PCDL500 and even 1,6-HDC and thus change the stoichiometry ratio within the reaction mixture and yield insoluble samples (Table S1). The reason behind the insolubility is the cross-linking of NIPU chains through the condensation reaction of urethane N–H groups arising from NIPU oligomers or unreacted 1,6-HDC with extra methylcarbamate (COOCH₃) groups.¹³

The progress of the transurethanization reaction was monitored via FTIR spectroscopy (Figure 1). The broad peak at 3349 cm⁻¹ in the FTIR spectrum of PCDL500, attributed to the stretching vibration of O–H bonds, significantly decreased (almost disappeared) in the FTIR spectrum of NIPU-D, preventatively, which means the consumption of the majority of hydroxyl groups in the course of the transurethanization reaction. The FTIR spectrum of NIPU-D displayed the characteristic peaks at 1732 and 1682

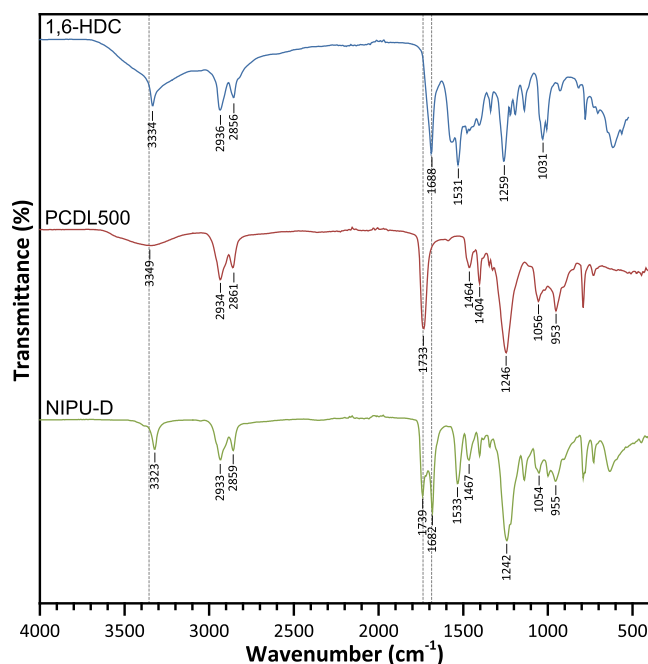


Figure 1. FTIR spectra of 1,6-HDC, PCDL500, and NIPU-D.

cm⁻¹ arising from the stretching vibration of C=O bonds of urethane and carbonate moieties in its backbone.

The chemical structure of NIPU-D was preventatively studied by NMR spectroscopy (Figures 2 and S1, S2 in Electronic Supporting Information, ESI). All peaks are assigned with the corresponding protons or carbons in the embedded molecular structure of NIPU-D. The protons of urethane moieties yielded a signal at 6.95 ppm. The protons at both α -positions of urethane moieties, that is, CH₂NHCO and NHCOCH₂, appeared at 3.06 and 3.97 ppm, respectively. Meanwhile, the carbons of urethane and carbonate moieties led to signals at 156.97 and 155.28 ppm. The carbons at both α -positions of urethane moieties, that is, CH₂NHCO and NHCOCH₂, appeared at 40.53 and 63.84 ppm, respectively. The NMR spectra confirmed the successful synthesis of NIPUs.

The thermal transitions of NIPUs were determined by DSC (Table 1 and Figure S3 in ESI). NIPUs displayed the thermal profile of semicrystalline polymers including glass transition, crystallization, and melting. The T_g of NIPUs was decreased from -28 to -41 °C by employing higher molecular weight PCDLs, which resulted in lower hard segment (urethane moieties) contents. The hard segments could physically cross-link the soft segments (carbonate moieties) through hydrogen bonds and limit their chain dynamics and free volume. NIPU-A and NIPU-D based on the lowest molecular weight PCDL and thus highest hard segment content displayed higher T_c and T_m values than NIPU-B and NIPU-C. The higher enthalpy

Table 1. GPC and DSC Data for NIPUs

NIPU	MW of PCDL (g/mol)	GPC			DSC						
		M_n (g/mol)	M_w (g/mol)	PDI	T_g (°C)	T_c (°C)	ΔH_c (J/g)	T_{cc} (°C)	ΔH_{cc} (J/g)	T_m (°C)	ΔH_m (J/g)
NIPU-A	500	14,200	26,200	1.85	-28	56	31.6	No	No	108	23.5
NIPU-D	500	24,300	58,600	2.41	-27	53	30.5	No	No	107	37.5
NIPU-B	1000	8800	14,500	1.64	-40	24	25.3	No	No	64	19.1
NIPU-C	2000	10,400	18,700	1.80	-41	-4	3.6	7	19.5	44	27.8

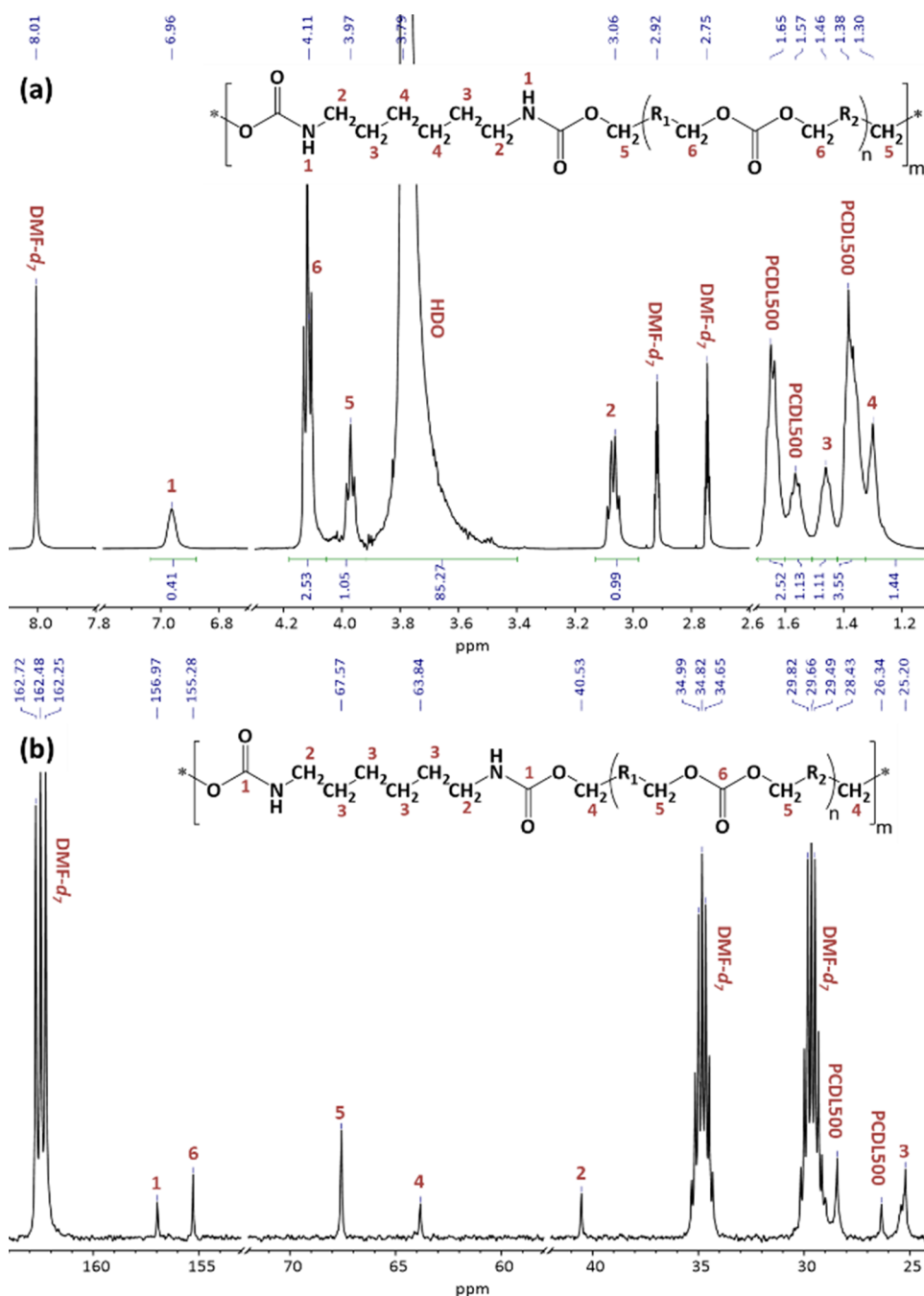


Figure 2. ^1H -NMR (a) and ^{13}C -NMR (b) spectra of NIPU-D in $\text{DMF-}d_7$.

(ΔH_c and ΔH_m) values for NIPU-A and NIPU-D displayed their higher crystallinity compared to NIPU-B and NIPU-C. NIPU-C, based on the highest molecular weight PCDL and hence with the lowest hard segment content, showed a low crystallization affinity because a very small crystallization peak ($\Delta H_c = 3.6 \text{ J/g}$) was detected during its cooling cycle and it mainly crystallized during the second heating cycle ($\Delta H_{cc} = 19.5 \text{ J/g}$). The double molecular weight of NIPU-D compared to NIPU-A did not significantly change the transition temperatures (T_g , T_c , and T_m) but improved its crystallinity ($\Delta H_m = 37.5 \text{ J/g}$ compared to $\Delta H_m = 23.5 \text{ J/g}$, respectively). All NIPUs presented two melting peaks in the first heating cycle and one melting peak in the second heating cycle (Figure S3 in ESI). It means the carbonate and urethane moieties

phase-separated over time to generate soft segments with lower T_m values (48–64 °C) and hard segments with higher T_m values (57–115 °C), respectively.

3.2. Electrospinning of NIPUs. Before electrospinning, the solubility of the NIPUs was tested. All NIPUs were soluble in DMF, THF, and HFIP: those with an M_w below 30,000 g/mol (NIPU-A, NIPU-B, and NIPU-C) up to a concentration of 50 wt % and those with a higher molecular weight (NIPU-D) usually up to 35 wt %. Meanwhile, NIPU-A and NIPU-D, both based on PCDL500, had a higher solubility in HFIP compared to DMF and THF. In the first step to establishing a stable electrospinning process, the electrospinnability of NIPU-A, NIPU-B, and NIPU-C was investigated in combination with different solvents (Figure S4 in ESI). Although the electro-

Table 2. Overview of the Established Electrospinning Parameters and Resulting Fiber Diameters^a

samples			electrospinning parameters						fiber diameter	
NIPU	conc.	salt	U (kV)	φ (mL/h)	CID (mm)	rH (%)	T (°C)	d (cm)	average (μm)	spread (μm)
NIPU-A	50%	no	20	0.1	0.5	30	40	25	— ^b	— ^b
NIPU-D	30%	no	19–24	0.2	0.5	30	40	28	1.05 \pm 0.23	0.46
NIPU-D	35%	no	24	0.2	0.5	30	40	28	2.42 \pm 0.01	0.59
NIPU-D	25%	yes	23	0.4	0.5	20	35	28	1.11 \pm 0.03	0.34
NIPU-D	30%	yes	22	0.4	0.5	20	35	28	1.23 \pm 0.23	0.36
NIPU-D	35%	yes	23	0.4	0.5	20	35	28	2.53 \pm 0.27	0.76

^a U : electrical potential, φ : flow speed, CID: cannula inner diameter, rH: relative humidity, T : temperature, and d : tip-to-collector distance. The average values refer to the mean of the fiber diameters and the inter-sample standard deviation ($n = 3$) and the spread refers to the mean of the standard deviation of the intra-sample fiber distributions. ^bThe electrospun sample contained beads.

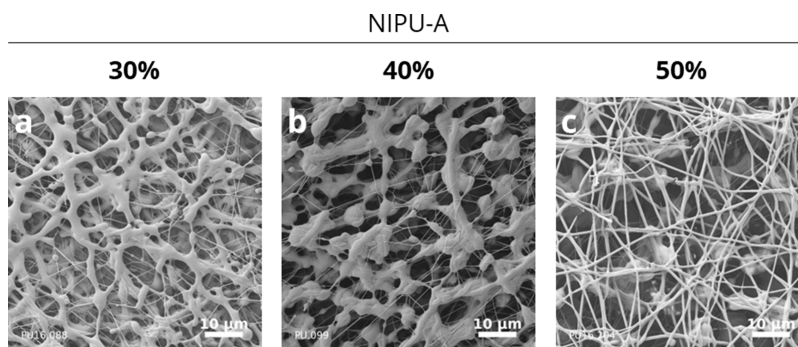


Figure 3. SEM micrographs of electrospun NIPU-A mats electrospun at 30 wt % (a), 40 wt % (b), and 50 wt % (c) in HFIP.

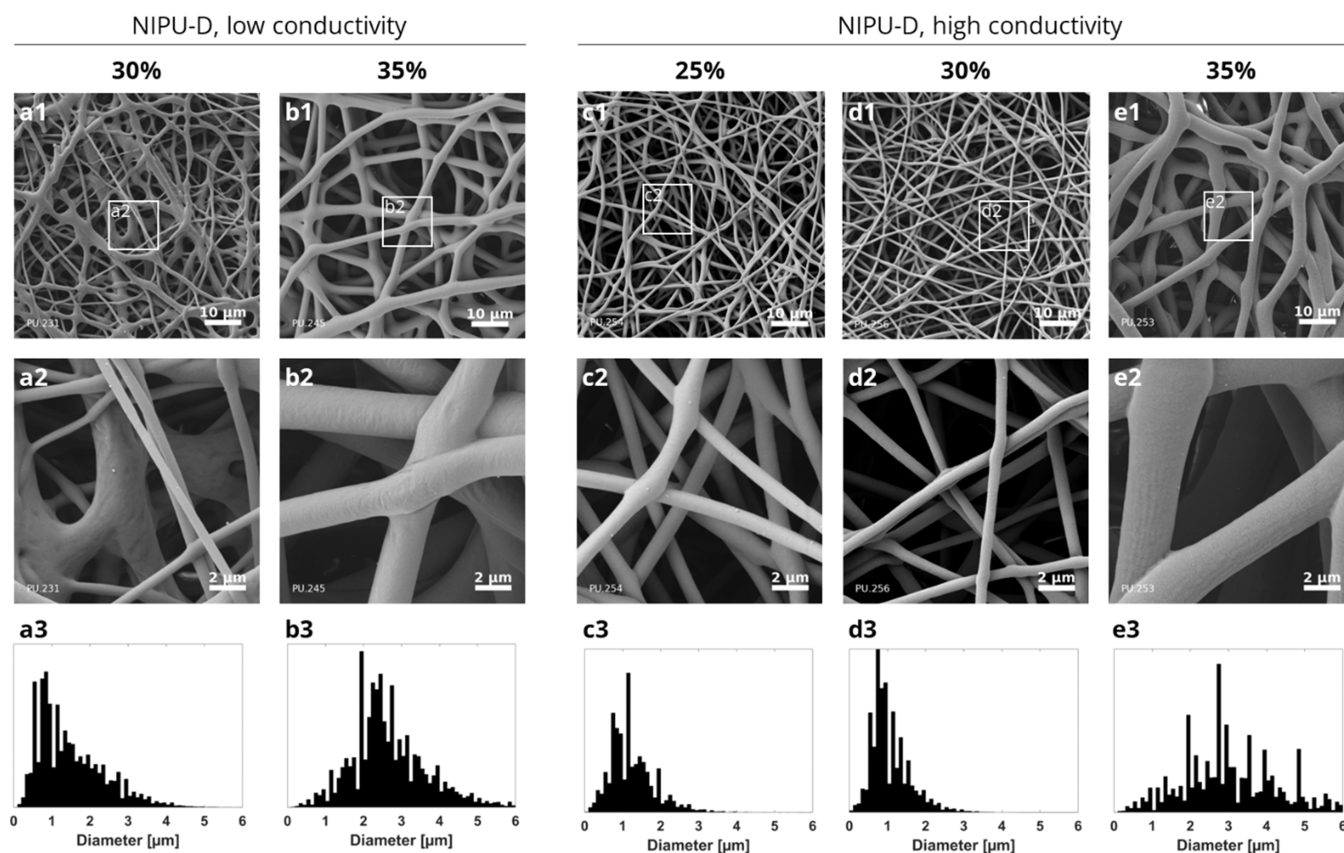


Figure 4. SEM micrographs and the corresponding intra-sample distribution of the fiber diameters of electrospun NIPU-D mats, which were electrospun at a concentration of 30 wt % (a) and 35 wt % (b) in HFIP with low conductivity ($<0.1 \mu\text{S}/\text{cm}$) and of those which were electrospun at a concentration of 25 wt % (c), 30 wt % (d), and 35 wt % (e) in HFIP with high conductivity ($10 \mu\text{S}/\text{cm}$).

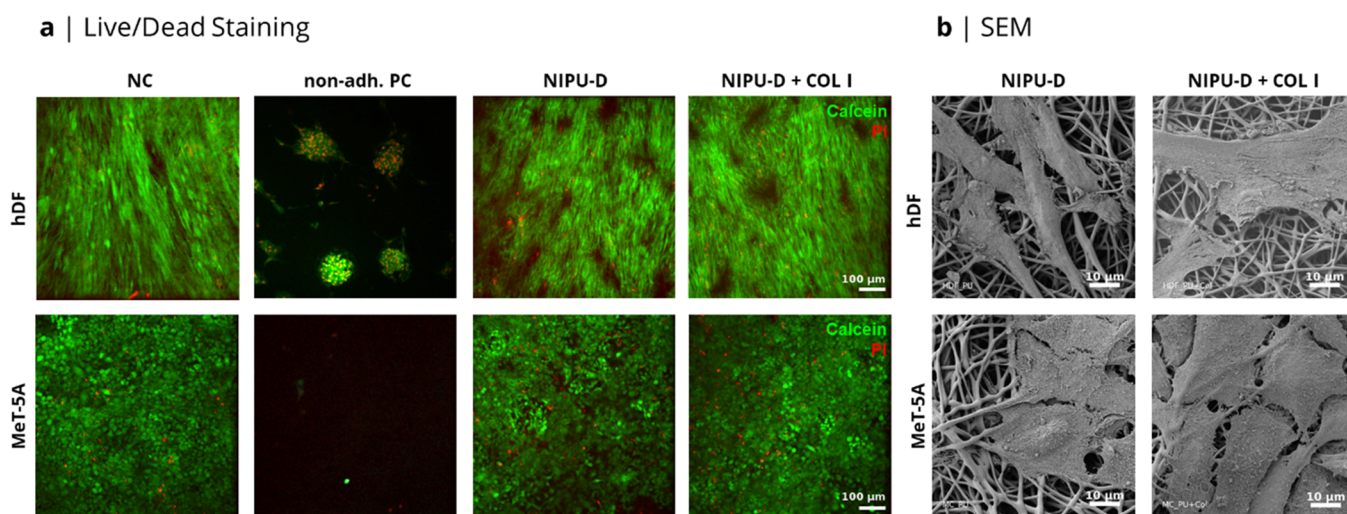


Figure 5. (a) Live/dead staining of hDFs and MeT-5A cells on electrospun NIPU-D mats after 7 days of static cell culture. (b) SEM images of hDFs and MeT-5A cells on electrospun NIPU-D mats after 24 h of static cell culture. NC: glass, non-adh. PC: Parafilm. Representative images from three independent experiments ($n = 3$).

spinning of NIPUs in DMF solutions yielded a small Taylor cone and a thin stable fiber (Figure S4b in ESI), there was no sign of a fibrous microstructure on the collector (Figure S4e in ESI). The electrospinning of NIPUs in THF solutions was considered to be unviable, as the relatively high vapor pressure of THF caused the solidification of the solutions at the tip of the cannula (Figure S4c in ESI), which prematurely halted the electrospinning process. Only electrospinning of NIPUs in HFIP solutions resulted in a partially fibrous scaffold (Figure S4d in ESI) when dissolved at concentrations of over 30 wt %. Because the electrospinning of NIPU-A based on PCDL 500 and with the highest molecular weight ($M_w = 26,200$ g/mol) in HFIP had shown the most promising results, further optimization of the electrospinning process was only conducted with HFIP as an electrospinning solvent.

High-molecular-weight NIPU-A ($M_w = 26,200$ g/mol) and NIPU-D ($M_w = 58,600$ g/mol), both based on PCDL500, were successfully electrospun into fibrous mats. An overview of the established electrospinning parameters that resulted in a stable fiber-yielding process and the corresponding average fiber diameters and spreads is listed in Table 2.

The formation of fibers during the electrospinning of NIPU-A started at a solution concentration of 30 wt % and improved with increasing the solution concentration up to 50 wt %, whilst the number of beads decreased (Figure 3). At the highest achieved concentration of 50 wt %, the NIPU-A mats were not bead-free. At higher concentrations (>50 wt %), the NIPU-A solutions became too viscous for electrospinning.

The first signs of fibers in NIPU-D mats started earlier at a solution concentration of 30 wt % with an average fiber diameter of 1.05 ± 0.23 μm . At a higher concentration (35 wt %), the fiber diameter increased to 2.42 ± 0.01 μm and the fiber morphology improved, as the formation of molten junctions decreased (Figure 4a,b). The reduction of bead formation and the increase in the fiber diameter in NIPUs with a higher molecular weight and solution concentration can be attributed to the rheological properties of the electrospinning solution, which have already been observed in the electrospinning of traditional TPUs⁴³ as well as other polymers.^{44–46} Moreover, the fibers in the NIPU-D mats had a more defined morphology compared to those in NIPU-A mats, which

strengthens the premise that higher molecular weights improve the electrospinnability of NIPUs. By increasing the solution conductivity to 10 $\mu\text{S}/\text{cm}$, via supplementing HFIP with sodium carbonate salt, the formation of fibers started at 25 wt % and slightly thickened at 30 wt % with fiber diameters being 1.11 ± 0.03 μm and 1.23 ± 0.28 μm . Compared to the NIPU mats electrospun out of unsupplemented HFIP, fibers were more separated and had more well-defined round cross-sections (Figure 4c,d). Furthermore, the intra-sample fiber diameter spread was narrowed and the fibrous mats contained a few molten fibers up to a concentration of 30 wt %. Because electrospinning of NIPU-D at 25 wt % in supplemented HFIP was found to be the most stable electrospinning process with the smallest intra-sample fiber diameter spread (0.34 ± 0.01 μm), these process parameters (Table 2) were selected for the creation of electrospun mats for biocompatibility tests.

3.3. Biocompatibility of Electrospun Mats. To assess the suitability of electrospun NIPU mats as a possible pericardial substitute in cardiac tissue engineering, the ability of the mats to facilitate the adhesion and proliferation of fibroblasts and epithelial cells was investigated in vitro. The relative viabilities for the L929 cells cultured in NIPUs' medium extracts were over 70% (Figure S5 in ESI); therefore, none of the synthesized NIPUs were considered to be cytotoxic. The electrospinning of NIPUs did not negatively affect the relative viability of the L929 cells in the medium extracts. It means that vacuum drying was sufficient to remove any remaining HFIP residues.

Most TPUs are known to be hydrophobic with no natural recognition sites for cells, which can hinder their application in tissue engineering. Therefore, their surfaces are commonly modified through the surface immobilization of biomolecules to improve the interfacial properties.⁴⁷ Here, the electrospun NIPU-D mats were functionalized with collagen to investigate the effect of biofunctionalization on biocompatibility. The collagen functionalization only minimally decreased the contact angle of mats from $101 \pm 6^\circ$ to $98 \pm 2^\circ$ (Figure S6 in ESI), although the immunological staining against collagen I confirmed the successful surface adsorption of collagen on the fibers (Figure S7 in ESI). The performance of the bare and collagen-functionalized electrospun NIPU-D mats was eval-

uated after 24 h and 7 days of static culture employing live/dead staining with calcein and PI (Figure 5a). The used MeT-5A (epithelial cells) originated from the pleural mesothelial membrane, comprising squamous epithelial cells. The same simple squamous epithelial cells line the outermost pericardial layer toward the serous cavity.^{48–50} After 24 h, both fibroblasts and epithelial cells stained predominantly positive for calcein, except for some scarcely distributed PI-positive epithelial cells on the bare mats. (Figure S8 in ESI). After 7 days, both cell types formed almost confluent cell layers and were almost exclusively stained calcein-positive on both mats.

Furthermore, the morphology and the arrangement of both cell types on the bare and collagen-functionalized electrospun NIPU mats reflected those on the negative control (glass) by this time point. The hDFs presented an almost confluent layer of spindle-shaped fibroblasts, whereas the MeT-5A cells showed an anticipated cobblestone morphology in a closely packed arrangement. As expected, the cells barely adhered to the nonadherent positive control (Parafilm). Both cell types displayed adhesion and interaction with the bare and collagen-functionalized electrospun NIPU mats by using their filopodia, which is observed in the SEM images (Figure 5b). Moreover, the SEM images revealed the cobblestone morphology of the epithelial cells and the tendency to form a closely packed single-cell layer. Despite the high contact angles, both mats provided a highly biocompatible substrate for the cultured cells. More specifically, the bare mats performed as well as the biofunctionalized mats, which shows that the electrospun NIPU mats can be very well employed as a three-dimensional scaffold without further processing. These biocompatibility studies indicate that the bare electrospun NIPU mats do not pose any adverse effects on cell proliferation and are an interesting candidate for use in tissue engineering applications. Although the comparison against a commercially available TPU was not considered in the present study, live/dead staining may not reveal increased biocompatibility in a direct comparison between NIPUs and conventional TPUs.⁸ TPUs generally owe their biocompatibility to their high stability, unless their hard-segment chemistry is modified to be more prone to hydrolytic degradation.^{51,52} Implanted biomaterials usually become subject to such hydrolytic activities during inflammatory responses, for example, through cholesterol esterase.^{53–55} To prevent the release of potentially harmful hard-segment degradation products, attempts have been made to replace aromatic diisocyanates in favor of aliphatic diisocyanates, for example, 1,6-butane diisocyanate (BDI), that are expected to yield naturally occurring degradation products, such as putrescine (1,4-butane diamine).⁵⁶ However, the use of aliphatic isocyanates, including BDI, highly increases the hydrolytic degradation rate, and the use of diisocyanates in the synthesis still poses a major health concern. Here, we showed that isocyanates and tin-based catalysts can be entirely eliminated in the production chain of electrospun TPU grafts, while the easy processability of TPU in electrospinning is retained. Still, the solubilization of these NIPUs required the use of HFIP, a fluorinated solvent, which is not quite devoid of safety concerns. Further risk reduction can be achieved by exploring electrospinning processes that do not require fluorinated solvents, such as solvent-free melt electrowriting, and hence further improve the sustainability of TPU graft production.

4. CONCLUSIONS

To reduce the environmental and human health dangers in the production of nonwoven PC-based TPU mats, it is key to establish a green synthesis route, which eliminates the use of isocyanates and tin-based catalysts. Here, we demonstrated a synthesis route through transurethanization with the use of 1,6-HDC and PCDLs with different molecular weights. The lower viscosity of PCDL500 and continuous stirring under reduced pressure aided the extraction of methanol and allowed for the synthesis of NIPUs with the highest molecular weights. The highest achieved molecular weight (M_w) was 58,600 g/mol, which proved to be sufficiently high for a fiber-yielding electrospinning process. Fiber formation was observed in PCDL500-based NIPUs with an M_w starting at 26,200 g/mol with increasing solution concentration and considerably improved in NIPU-D with an even higher M_w of 58,600 g/mol. Despite high water contact angles, the bare electrospun NIPU mats did not underperform in comparison to collagen-functionalized mats because both fibroblasts and epithelial cells displayed good adhesion and proliferation. These in vitro investigations of the electrospun NIPU mats showed that they bear great potential in biomimetic cardiac scaffolds.

■ ASSOCIATED CONTENT

Supporting Information

The Supporting Information is available free of charge at <https://pubs.acs.org/doi/10.1021/acsomega.2c03731>.

¹H-NMR spectrum for PCDL500 in CDCl₃; ¹H-NMR spectrum for 1,6-HDC in CDCl₃; reaction parameters for the synthesis of NIPUs; DSC curves of NIPUs; optical and SEM images for the electrospinning of NIPUs with different electrospinning solvents; relative viability of L929 cells in medium extracts of NIPUs assessed using MTT assay; contact angle for water droplets on electrospun NIPU-D mats; and collagen immunostaining and live/dead staining (PDF)

■ AUTHOR INFORMATION

Corresponding Authors

Dmitri Visser – NMI Natural and Medical Science Institute at the University of Tübingen, 72770 Reutlingen, Germany; orcid.org/0000-0002-8868-9265; Phone: +49 (0) 7121 51530-292; Email: dmitri.visser@nmi.de

Hadi Bakhshi – Department of Life Science and Bioprocesses and Department of Functional Polymer Systems, Fraunhofer Institute for Applied Polymer Research IAP, 14476 Potsdam, Germany; Phone: +49 (0) 331-568-1425; Email: hadi.bakhshi@iap.fraunhofer.de

Authors

Katharina Rogg – NMI Natural and Medical Science Institute at the University of Tübingen, 72770 Reutlingen, Germany

Ellena Fuhrmann – NMI Natural and Medical Science Institute at the University of Tübingen, 72770 Reutlingen, Germany

Franziska Wieland – Department of Functional Polymer Systems, Fraunhofer Institute for Applied Polymer Research IAP, 14476 Potsdam, Germany

Katja Schenke-Layland – NMI Natural and Medical Science Institute at the University of Tübingen, 72770 Reutlingen, Germany; Institute of Biomedical Engineering, Dept. for Medical Technologies and Regenerative Medicine and Cluster

of Excellence iFIT (EXC 2180) "Image-Guided and Functionally Instructed Tumor Therapies", Eberhard Karls University Tübingen, 72076 Tübingen, Germany; orcid.org/0000-0001-8066-5157

Wolfdietrich Meyer – Department of Life Science and Bioprocesses and Department of Functional Polymer Systems, Fraunhofer Institute for Applied Polymer Research IAP, 14476 Potsdam, Germany; orcid.org/0000-0003-1330-2887

Hanna Hartmann – NMI Natural and Medical Science Institute at the University of Tübingen, 72770 Reutlingen, Germany; orcid.org/0000-0001-9643-998X

Complete contact information is available at:
<https://pubs.acs.org/10.1021/acsomega.2c03731>

Notes

The authors declare no competing financial interest. hDFs were isolated from juvenile foreskin under ethics approval no 495/2018BO2 from the University Hospital of Tübingen, Germany.

ACKNOWLEDGMENTS

The authors acknowledge the financial support by the Federal Ministry of Education and Research of Germany in the framework of "ProMatLeben – Polymere" (project numbers 13XP5087D and 13XP5087E, PolyKARD). Furthermore, the authors are grateful to Birgit Schröppel (NMI Centre for Nanoanalytics) for her technical support with SEM and critical point drying, Xin Xiong for his support in the rat-tail collagen isolation, and Svenja Reimer for the original PolyKARD draft.

REFERENCES

- (1) Lockey, J. E.; Redlich, C. A.; Streicher, R.; Pfahles-Hutchens, A.; Hakkinen, P. J.; Ellison, G. L.; Harber, P.; Utell, M.; Holland, J.; Comai, A.; White, M. Isocyanates and human health: Multi-stakeholder information needs and research priorities. *J. Occup. Environ. Med.* **2015**, *57*, 44.
- (2) Redlich, C.; Bello, D.; Wisniewski, A.; Health effects of isocyanates. In *Environmental and occupational medicine*, 4th ed.; Rom, W.; Markowitz, S.; Eds., Lippincott Williams & Wilkins, 2007; pp 502–515.
- (3) Allport, D. C.; Gilbert, D. S.; Outterside, S.; *MDI and TDI: safety, health and the environment: a source book and practical guide*. John Wiley & Sons, 2003.
- (4) Gagné, S.; Lesage, J.; Ostiguy, C.; Van Tra, H. Determination of unreacted 2,4-toluene diisocyanate (2,4TDI) and 2,6-toluene diisocyanate (2,6TDI) in foams at ultratrace level by using HPLC-CIS-MS-MS. *Analyst* **2003**, *128*, 1447–1451.
- (5) Krone, C. A.; Ely, J. T. A.; Klingner, T.; Rando, R. J. Isocyanates in flexible polyurethane foams. *Bull. Environ. Contam. Toxicol.* **2003**, *70*, 328–335.
- (6) Nath, M. Toxicity and the cardiovascular activity of organotin compounds: A review. *Appl. Organomet. Chem.* **2008**, *22*, 598–612.
- (7) Tanzi, M. C.; Verderio, P.; Lampugnani, M. G.; Resnati, M.; Dejana, E.; Sturani, E. Cytotoxicity of some catalysts commonly used in the synthesis of copolymers for biomedical use. *J. Mater. Sci.: Mater. Med.* **1994**, *5*, 393–396.
- (8) Aduba, D. C.; Zhang, K.; Kanitkar, A.; Serrine, J. M.; Verbridge, S. S.; Long, T. E. Electrospinning of plant oil-based, non-isocyanate polyurethanes for biomedical applications. *J. Appl. Polym. Sci.* **2018**, *135*, 46464.
- (9) Pramanik, S. K.; Sreedharan, S.; Singh, H.; Khan, M.; Tiwari, K.; Shiras, A.; Smythe, C.; Thomas, J. A.; Das, A. Mitochondria targeting non-isocyanate-based polyurethane nanocapsules for enzyme-triggered drug release. *Bioconjugate Chem.* **2018**, *29*, 3532–3543.
- (10) Zhao, Y.; Xia, X.; Zhou, J.; Huang, Z.; Lei, F.; Tan, X.; Yu, D.; Zhu, Y.; Xu, H. Thermoresponsive behavior of non-isocyanate poly(hydroxyl)urethane for biomedical composite materials. *Adv. Compos. Hybrid Mater.* **2021**, *5*, 843–852.
- (11) Ghasemlou, M.; Daver, F.; Ivanova, E. P.; Adhikari, B. Synthesis of green hybrid materials using starch and non-isocyanate polyurethanes. *Carbohydr. Polym.* **2020**, *229*, No. 115535.
- (12) Matsumoto, K.; Kokai, A.; Endo, T. Synthesis and properties of novel poly(hydroxyurethane) from difunctional alicyclic carbonate and m-xylolenediamine and its possibility as gas barrier materials. *Polym. Bull.* **2016**, *73*, 677–686.
- (13) Shen, Z.; Zhang, J.; Zhu, W.; Zheng, L.; Li, C.; Xiao, Y.; Liu, J.; Wu, S.; Zhang, B. A solvent-free route to non-isocyanate poly-(carbonate urethane) with high molecular weight and competitive mechanical properties. *Eur. Polym. J.* **2018**, *107*, 258–266.
- (14) Deng, Y.; Li, S.; Zhao, J.; Zhang, Z.; Zhang, J.; Yang, W. Crystallizable and tough aliphatic thermoplastic poly(ether urethane)s synthesized through a non-isocyanate route. *RSC Adv.* **2014**, *4*, 43406–43414.
- (15) Wolosz, D.; Parzuchowski, P. G.; Świdorska, A. Synthesis and characterization of the non-isocyanate poly(carbonate-urethane)s obtained via polycondensation route. *Eur. Polym. J.* **2021**, *155*, No. 110574.
- (16) Khan, I.; Smith, N.; Jones, E.; Finch, D. S.; Cameron, R. E. Analysis and evaluation of a biomedical polycarbonate urethane tested in an in vitro study and an ovine arthroplasty model. Part I: Materials selection and evaluation. *Biomaterials* **2005**, *26*, 621–631.
- (17) Doshi, J.; Reneker, D. H. Electrospinning process and applications of electrospun fibers. *J. Electrostat.* **1995**, *35*, 151–160.
- (18) Liu, Y.; Teng, H.; Hou, H.; You, T. Nonenzymatic glucose sensor based on renewable electrospun Ni nanoparticle-loaded carbon nanofiber paste electrode. *Biosens. Bioelectron.* **2009**, *24*, 3329–3334.
- (19) Lee, J. S.; Kwon, O. S.; Park, S. J.; Park, E. Y.; You, S. A.; Yoon, H.; Jang, J. Fabrication of ultrafine metal-oxide-decorated carbon nanofibers for DMMP sensor application. *ACS Nano* **2011**, *5*, 7992–8001.
- (20) Mercante, L. A.; Scagion, V. P.; Migliorini, F. L.; Mattoso, L. H. C.; Correa, D. S. Electrospinning-based (bio)sensors for food and agricultural applications: A review. *TrAC, Trends Anal. Chem.* **2017**, *91*, 91–103.
- (21) Lu, T.; Cui, J.; Qu, Q.; Wang, Y.; Zhang, J.; Xiong, R.; Ma, W.; Huang, C. Multistructured electrospun nanofibers for air filtration: a review. *ACS Appl. Mater. Interfaces* **2021**, *13*, 23293–23313.
- (22) Lv, D.; Zhu, M.; Jiang, Z.; Jiang, S.; Zhang, Q.; Xiong, R.; Huang, C. Green electrospun nanofibers and their application in air filtration. *Macromol. Mater. Eng.* **2018**, *303*, No. 1800336.
- (23) Khorshidi, S.; Solouk, A.; Mirzadeh, H.; Mazinani, S.; Lagaron, J. M.; Sharifi, S.; Ramakrishna, S. A review of key challenges of electrospun scaffolds for tissue-engineering applications. *J. Tissue Eng. Regen. Med.* **2016**, *10*, 715–738.
- (24) Arab-Ahmadi, S.; Irani, S.; Bakhshi, H.; Atyabi, F.; Ghalandari, B. Immobilization of cobalt-loaded laponite/carboxymethyl chitosan on polycaprolactone nanofiber for improving osteogenesis and angiogenesis activities. *Polym. Adv. Technol.* **2021**, *32*, 4362–4372.
- (25) Arab-Ahmadi, S.; Irani, S.; Bakhshi, H.; Atyabi, F.; Ghalandari, B. Immobilization of carboxymethyl chitosan/laponite on polycaprolactone nanofibers as osteoinductive bone scaffolds. *Polym. Adv. Technol.* **2021**, *32*, 755–765.
- (26) Orafa, Z.; Irani, S.; Zamanian, A.; Bakhshi, H.; Nikukar, H.; Ghalandari, B. Coating of laponite on PLA nanofibrous for bone tissue engineering application. *Macromol. Res.* **2021**, *29*, 191–198.
- (27) Lamba, N. M. K.; Woodhouse, K. A.; Cooper, S. L.; The Chemistry of Polyurethane Copolymers. In *Polyurethanes in Biomedical Applications*, 1st ed.; CRC Press, 2017; pp 5–25.
- (28) Kucinska-Lipka, J.; Gubanska, I.; Janik, H.; Sienkiewicz, M. Fabrication of polyurethane and polyurethane based composite fibres by the electrospinning technique for soft tissue engineering of cardiovascular system. *Mater. Sci. Eng., C* **2015**, *46*, 166–176.

- (29) Kidoaki, S.; Kwon, I. K.; Matsuda, T. Mesoscopic spatial designs of nano- and microfiber meshes for tissue-engineering matrix and scaffold based on newly devised multilayering and mixing electrospinning techniques. *Biomaterials* **2005**, *26*, 37–46.
- (30) Baudis, S.; Ligon, S. C.; Seidler, K.; Weigel, G.; Grasl, C.; Bergmeister, H.; Schima, H.; Liska, R. Hard-block degradable thermoplastic urethane-elastomers for electrospun vascular prostheses. *J. Polym. Sci., Part A: Polym. Chem.* **2012**, *50*, 1272–1280.
- (31) Daum, R.; Visser, D.; Wild, C.; Kutuzova, L.; Schneider, M.; Lorenz, G.; Weiss, M.; Hinderer, S.; Stock, U. A.; Seifert, M.; Schenke-Layland, K. Fibronectin adsorption on electrospun synthetic vascular grafts attracts endothelial progenitor cells and promotes endothelialization in dynamic in vitro culture. *Cell* **2020**, *9*, 778.
- (32) Stankus, J. J.; Guan, J.; Fujimoto, K.; Wagner, W. R. Microintegrating smooth muscle cells into a biodegradable, elastomeric fiber matrix. *Biomaterials* **2006**, *27*, 735–744.
- (33) Uttayarat, P.; Perets, A.; Li, M.; Pimton, P.; Stachelek, S. J.; Alferiev, I.; Composto, R. J.; Levy, R. J.; Lelkes, P. I. Micropatterning of three-dimensional electrospun polyurethane vascular grafts. *Acta Biomater.* **2010**, *6*, 4229–4237.
- (34) Amoroso, N. J.; D'Amore, A.; Hong, Y.; Rivera, C. P.; Sacks, M. S.; Wagner, W. R. Microstructural manipulation of electrospun scaffolds for specific bending stiffness for heart valve tissue engineering. *Acta Biomater.* **2012**, *8*, 4268–4277.
- (35) Puperi, D. S.; Kishan, A.; Punske, Z. E.; Wu, Y.; Cosgriff-Hernandez, E.; West, J. L.; Grande-Allen, K. J. Electrospun polyurethane and hydrogel composite scaffolds as biomechanical mimics for aortic valve tissue engineering. *ACS Biomater. Sci. Eng.* **2016**, *2*, 1546–1558.
- (36) Motiwale, S.; Russell, M. D.; Conroy, O.; Carruth, J.; Wancura, M.; Robinson, A.; Cosgriff-Hernandez, E.; Sacks, M. S. Anisotropic elastic behavior of a hydrogel-coated electrospun polyurethane: Suitability for heart valve leaflets. *J. Mech. Behav. Biomed. Mater.* **2022**, *125*, No. 104877.
- (37) Şenel Ayaz, H. G.; Perets, A.; Ayaz, H.; Gilroy, K. D.; Govindaraj, M.; Brookstein, D.; Lelkes, P. I. Textile-templated electrospun anisotropic scaffolds for regenerative cardiac tissue engineering. *Biomaterials* **2014**, *35*, 8540–8552.
- (38) D'Amore, A.; Yoshizumi, T.; Luketich, S. K.; Wolf, M. T.; Gu, X.; Cammarata, M.; Hoff, R.; Badylak, S. F.; Wagner, W. R. Bi-layered polyurethane – Extracellular matrix cardiac patch improves ischemic ventricular wall remodeling in a rat model. *Biomaterials* **2016**, *107*, 1–14.
- (39) Tao, Z. W.; Jarrell, D. K.; Robinson, A.; Cosgriff-Hernandez, E. M.; Jacot, J. G. A prevascularized polyurethane-reinforced fibrin patch improves regenerative remodeling in a rat right ventricle replacement model. *Adv. Healthcare Mater.* **2021**, *10*, No. 2101018.
- (40) Sun, D. L.; Xie, S. J.; Deng, J. R.; Huang, C. J.; Ruckenstein, E.; Chao, Z. S. CH₃COONa as an effective catalyst for methoxycarbonylation of 1,6-hexanediamine by dimethyl carbonate to dimethylhexane-1,6-dicarbamate. *Green Chem.* **2010**, *12*, 483–449.
- (41) Stadelmann, K.; Weghofer, A.; Urbanczyk, M.; Maulana, T. I.; Loskill, P.; Jones, P. D.; Schenke-Layland, K. Development of a bi-layered cryogenic electrospun polylactic acid scaffold to study calcific aortic valve disease in a 3D co-culture model. *Acta Biomater.* **2022**, *140*, 364–378.
- (42) Murphy, R.; Turcott, A.; Banuelos, L.; Dowey, E.; Goodwin, B.; Cardinal, K. O. SIMPoly: A matlab-based image analysis tool to measure electrospun polymer scaffold fiber diameter. *Tissue Eng., Part C* **2020**, *26*, 628–636.
- (43) Mi, H.-Y.; Jing, X.; Jacques, B. R.; Turng, L.-S.; Peng, X.-F. Characterization and properties of electrospun thermoplastic polyurethane blend fibers: Effect of solution rheological properties on fiber formation. *J. Mater. Res.* **2013**, *28*, 2339–2350.
- (44) Veleirinho, B.; Rei, M. F.; Lopes-Da-Silva, J. A. Solvent and concentration effects on the properties of electrospun poly(ethylene terephthalate) nanofiber mats. *J. Polym. Sci., Part B: Polym. Phys.* **2008**, *46*, 460–471.
- (45) Filip, P.; Peer, P. Characterization of poly(ethylene oxide) nanofibers—mutual relations between mean diameter of electrospun nanofibers and solution characteristics. *Processes* **2019**, *7*, 948.
- (46) Kim, K. W.; Lee, K. H.; Khil, M. S.; Ho, Y. S.; Kim, H. Y. The effect of molecular weight and the linear velocity of drum surface on the properties of electrospun poly (ethylene terephthalate) non-wovens. *Fibers Polym.* **2004**, *5*, 122–127.
- (47) Ren, X.; Feng, Y.; Guo, J.; Wang, H.; Li, Q.; Yang, J.; Hao, X.; Lv, J.; Ma, N.; Li, W. Surface modification and endothelialization of biomaterials as potential scaffolds for vascular tissue engineering applications. *Chem. Soc. Rev.* **2015**, *44*, 5680–5742.
- (48) Whitaker, D.; Papadimitriou, J. M.; Walters, M. N. I. The mesothelium and its reactions: A review. *Crit. Rev. Toxicol.* **1982**, *10*, 81–144.
- (49) Mutsaers, S. E. The mesothelial cell. *Int. J. Biochem. Cell Biol.* **2004**, *36*, 9–16.
- (50) Lachaud, C. C.; Rodriguez-Campins, B.; Hmadcha, A.; Soria, B. Use of mesothelial cells and biological matrices for tissue engineering of simple epithelium surrogates. *Front. Bioeng. Biotechnol.* **2015**, *3*, 117.
- (51) Tanzi, M. C.; Mantovani, D.; Petrini, P.; Guidoin, R.; Laroche, G. Chemical stability of polyether urethanes versus polycarbonate urethanes. *J. Biomed. Mater. Res.* **1997**, *36*, 550–559.
- (52) Santerre, J.; Woodhouse, K.; Laroche, G.; Labow, R. Understanding the biodegradation of polyurethanes: from classical implants to tissue engineering materials. *Biomaterials* **2005**, *26*, 7457–7470.
- (53) Christenson, E. M.; Patel, S.; Anderson, J. M.; Hiltner, A. Enzymatic degradation of poly (ether urethane) and poly (carbonate urethane) by cholesterol esterase. *Biomaterials* **2006**, *27*, 3920–3926.
- (54) Labow, R. S.; Meek, E.; Santerre, J. P. Synthesis of cholesterol esterase by monocyte-derived macrophages: a potential role in the biodegradation of poly (urethane) s. *J. Biomater. Appl.* **1999**, *13*, 187–205.
- (55) Tang, Y.; Labow, R.; Santerre, J. Enzyme-induced biodegradation of polycarbonate-polyurethanes: Dependence on hard-segment chemistry. *J. Biomed. Mater. Res.* **2001**, *57*, 597–611.
- (56) Guan, J.; Fujimoto, K. L.; Sacks, M. S.; Wagner, W. R. Preparation and characterization of highly porous, biodegradable polyurethane scaffolds for soft tissue applications. *Biomaterials* **2005**, *26*, 3961–3971.